Diffusion path and Haven's ratio of mobile ions in α-Ag_2Te

M. Kobayashi and K. Ishikawa
Department of Physics, Niigata University, Ikarashi, Niigata 950-21, Japan

F. Tachibana
Information Processing Center, Niigata University, Ikarashi, Niigata 950-21, Japan

H. Okazaki
Department of General Education, Niigata University, Ikarashi Niigata 950-21, Japan
(Received 9 December 1987; revised manuscript received 24 March 1988)

A molecular-dynamics method is applied in a study of silver diffusion in superionic conductor Ag_2Te for several temperatures with use of effective pairwise potentials. The static and dynamical structures are calculated. The density distribution map of silver ions suggests that a Ag ion, located at a tetrahedral site for most of the time, moves to a neighboring tetrahedral site via the vicinity of an octahedral site—a result which is consistent with the explanation of Haven's ratio proposed by Okazaki. The activation energy for a ionic diffusion also is obtained from the Arrhenius plotting of the self-diffusion coefficient of Ag^+.

I. INTRODUCTION

Superionic conductors are characterized by their highly ionic conduction compared with that of a liquid electrolyte. Many electronic and ionic properties, such as the conductivity, Hall coefficient, and thermoelectric power, and galvano-magnetic and thermomagnetic behaviors, of the superionic conductor α-Ag_2Te have been measured by Miyatani.[1] To explain many of the above-mentioned experimental observations, Yokota has developed a macroscopic theory of mixed conduction which includes electronic and ionic conduction. He also proposed a theory[2] of a caterpillar mechanism of mobile ions in the superionic conductors to interpret the remarkable deviation from the Einstein relation in silver chalcogenides, which was observed by one of the present authors.[3] Many authors have tried to construct realistic models to explain the characteristics of superionic conductors.[4] The major difficulty in so doing is to determine a way to take into account the anharmonicity of lattice ions. Inclusion of the effects due to collective motion of mobile ions is even more difficult.

Recently, molecular-dynamics (MD) calculations have been used for the study of condensed-matter systems.[5] Rahman and Vashishta[6] have succeeded in describing the nature of ionic motions in AgI and CuI using MD techniques.

We have studied structural and dynamical properties of the superionic conductor Ag_2Te using MD simulation. The MD method provides us a microscopic picture of the diffusion process of silver ions in a system. The calculations presented are based on the assumption that Newton's equation of motion with a two-body central-force interaction can give a reasonable description of the motion of ions in α-Ag_2Te. In practical computations, the following restrictions are imposed: (1) the interaction potentials have to be restricted to the main terms, namely the soft-core repulsive interaction and Coulomb interaction, and (2) the number of particles in the system has to be kept rather small, as for a 324-particle system.

II. METHOD OF COMPUTATION

The soft-core repulsive potential is quite important in a description of the thermodynamic properties of inert gases, alkali metals, and alkaline-earth metals.[7] This potential also plays an important role in characterizing the dynamic properties of a high-density monatomic classical liquid. When we consider the superionic conductor system, we have to include the Coulomb potential in addition to the soft-core potential. For Ag_2Te we use the following effective pairwise potential:

$$\Phi_{ij}(r)=A_{ij}\left[\frac{\sigma_i+\sigma_j}{r}\right]^n+\frac{z_i z_j e^2}{r}\ , \tag{1}$$

where i,j describe the type of ions, A_{ij} the repulsive strength, σ_i,σ_j the particle radii, z_i,z_j the effective valence, and e the elementary charge. We assume $A_{ij}=A$. The values of σ_{Te} and σ_{Ag} are determined so as to avoid the overlapping of ions, that is, these are defined as follows:

$$\sigma_{Te}+\sigma_{Te}=\text{Te-Te nearest-neighbor distance}\ ,$$

$$\sigma_{Te}+\sigma_{Ag}=\text{Te-Ag nearest-neighbor distance}\ .$$

If the fcc lattice constant is taken to be 6.6 Å, we get $\sigma_{Te}=2.21$ Å and $\sigma_{Ag}=0.65$ Å, assuming the Ag positions to be the tetrahedral sites of the fcc lattice. We take $n=7$ so as to realize the crystal stability overcoming the van der Waals potential, which is not included in Eq. (1), for the particle contact. The values of other parameters used are as follows:

$$A=0.1\ \text{eV},\quad z_{Te}=-2z_{Ag}=-1.1\ .$$

These values are chosen so as to reproduce the diffusion constant at 550 K and the ionic conductivity of Ag_2Te measured by Miyatani[1] and Okazaki.[8] The simulation gives reasonable values for the cohesive energy U, compressibility κ, and elastic constants C_{11}, C_{12} as follows:

$$U = 46.4 \text{ kcal/mol} ,$$

$$\kappa = 5.71 \times 10^{-11} \text{ cm}^3/\text{erg} ,$$

$$C_{11} = 1.74 \times 10^{11} \text{ dyn/cm}^2 ,$$

$$C_{12} = 0.235 \times 10^{11} \text{ dyn/cm}^2 .$$

The calculations were performed on a 324-particle system in a cubic cell 19.8 Å long in which the Te ions form a fcc lattice with the lattice constant 6.6 Å. Coulomb interactions were calculated with use of the Ewald summations.[5,6] The integration time step was 9.3×10^{-15} s. In order to avoid the surface effects, the usual periodic boundary conditions were imposed on the system. The calculation was initiated by allocating the Te ions on the fcc lattice points and the Ag ions on the tetrahedral sites. Since we did sufficiently long initial aging, of the system, namely 1000 time steps, the starting conditions have no effect on the results reported here. For the calculations of the average quantities of interest, 12 000 time steps were performed. The calculations were carried out for several temperatures.

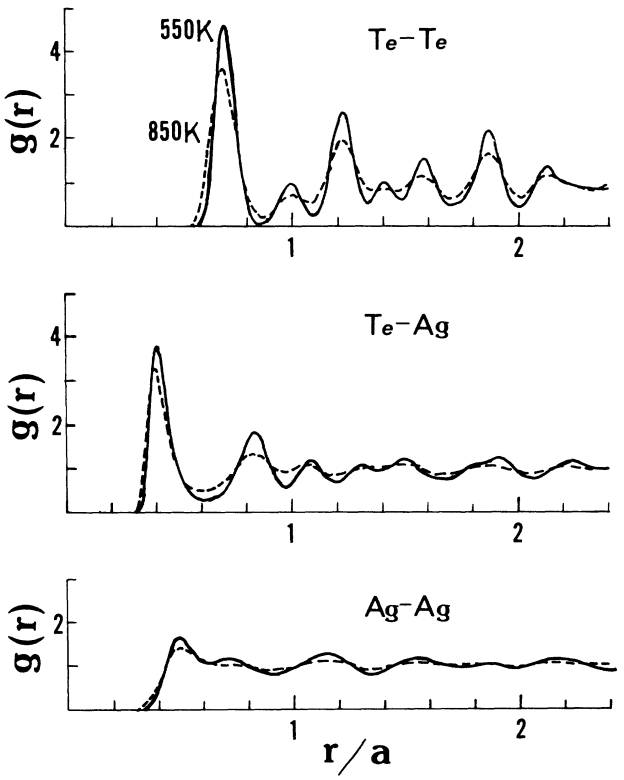

FIG. 1. Radial distribution functions at two temperatures, 550 K (solid line) and 850 K (dotted line). The transverse axis is scaled by the lattice constant a.

III. RESULTS AND DISCUSSION

A. Radial distribution functions

For a one-component system, the radial distribution function $g(r)$ is related to $n(r)\delta r$, the average number of particles at distances between r and $r+\delta r$ from a given particle, by

$$g(r) = \frac{V}{N} \frac{n(r)}{4\pi r^2} , \tag{2}$$

where V is the volume of the box containing the N particles and $n(r)$ is the number density. The extension of this definition to the partial radial distribution functions for our system is obvious, e.g., $g_{\text{Te-Ag}}(r)$ is defined by placing a Te ion at the origin and restricting $n(r)$ to Ag ions. A similar definition is given to $g_{\text{Ag-Ag}}(r)$ and $g_{\text{Te-Te}}(r)$. These radial distribution functions, $g_{\text{Te-Te}}(r)$, $g_{\text{Te-Ag}}(r)$, and $g_{\text{Ag-Ag}}(r)$, are shown in Fig. 1 at two different temperatures, 550 K (solid line) and 850 K (dotted line). From these figures we see a proper configuration of ions, namely, the Te ions from a well-defined fcc structure and the Ag ions are distributed in liquid as at tetrahedral sites.

B. Density distribution of Ag ions.

Since the Te ions form a well-defined fcc structure, it is reasonable to use its lattice as a reference frame to see the position of the Ag ions. The most interesting region is a (110) plane of the lattice and the presence of Ag ions in a block of thickness $\sqrt{2}a/16$ (=0.58 Å, a is the lattice constant). The block is shown in the solid lines in Fig. 2 and is divided into 32×32 rectangular pieces with the $(\sqrt{2}a/32) \times (a/32)$ as shown in Fig. 2. The number of Ag ions included in each piece is calculated and is averaged over time. Points B and C are the tetrahedral and the octahedral site, respectively. The Ag-ion density distribution on the (110) plane at 850 K is shown in Fig. 3. A, B, C, D, and E express the corresponding positions shown in Fig. 2.

Figure 4 shows the Ag-ion density distribution on the $(\frac{1}{4}00)$ plane. The Ag-ion distribution at point E is zero. Then the migration of Ag ions does not take place through point E, i.e., Ag ions do not move from one tetrahedral site to another directly.

Figures 3 and 4 suggest that Ag ion stays at the tetrahedral site for most of the time and moves to its neighboring tetrahedral site through the vicinity of the octahedral site. The calculated Ag distribution supports the jump-diffusion mechanism of cations along the wavy lines consisting of alternating tetrahedral and octahedral sites in the (110) plane, as suggested by Okazaki.[3] This result is compared with the x-ray data.[9]

Koto, Schulz, and Huggins[10] have made x-ray-diffraction measurements on PbF_2. They have found that the diffusive F^- ions left from one of the tetrahedral sites through the tetrahedral faces and moved through the octahedron in the center of the unit cell and then returned to a tetahedral site. There was no pronounced local potential minima along the diffusion path of F^- ions. Our

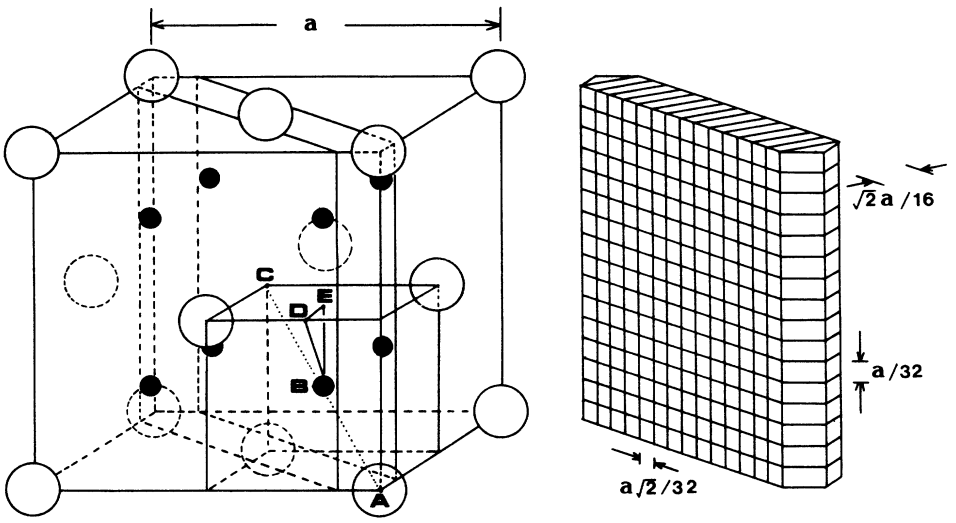

FIG. 2. Antifluorite structure. Open circles show the fcc anion (Te) lattice sites and the solid circles show the tetrahedral sites. Points B and C are the tetrahedral and octahedral sites, respectively. The parameter a is the lattice constant.

result for the diffusion path of Ag^+ agrees with their results.

Now we have to refer to the results found by simulation and other experiments in PbF_2. The neutron-diffraction work by Dickens *et al.*[11] and simulation studies by Walker, Dixon, and Gillan[12] and Gillan[13] have shown that the diffusion of the F^- ion in PbF_2 occurs by direct jumps between the tetrahedral sites. PbF_2 and Ag_2Te have the same structure. However, PbF_2 differs from Ag_2Te in that the immobile sublattice is the same in the low- and high-temperature phases and mobile sublattice disordering occurs gradually with increasing temperature. On the other hand, there is a rearrangement of the immobile-ion sublattice at the superionic phase-transition temperature, T_c, in addition to the disordering of the mobile ion sublattice in AgI-type superionic conductors. Moreover, the mobile ions in PbF_2 are F^- anions and those in Ag_2Te are Ag^+ cations. This difference yields, consequently, a different path for the diffusion of mobile ions. In addition to these it is worth mentioning that the effective sizes of these mobile ions are quite different, as discussed below. We define the ratio of ionic radii as follows: ρ is the ratio of the ionic radius of the immobile ion to the ionic radius of the mobile ion. If we use the values of the ionic radii by Pauling, the ratio γ is about unity for PbF_2 and 1.6 for Ag_2Te. For the present MD calculations we take $\rho=3.4$. A high value of ρ will offer a space which is available to the diffusion. Furthermore, the mass ratios of these materials are $m_{Ag}/m_{Te}=0.845$ and $m_F/m_{Pb}=0.092$. Then it is reasonable to say that very great differences in both the ratio ρ and mass ratio have a great influence on the dynamical properties of these materials: diffusing path, ionic conductivity, etc. The same discussion is given in recent simulation work on CaF_2 by Kaneko and Ueda.[14]

C. Mean-square displacement

The mean-square displacement (MSD) for anions and cations is defined by

$$\langle r^2(t)\rangle_\alpha=\frac{1}{N_\alpha}\sum_{i=1}^{N_\alpha}\langle\,|\mathbf{r}_i(t)-\mathbf{r}_i(0)|^2\rangle,\quad \alpha=\pm \tag{3}$$

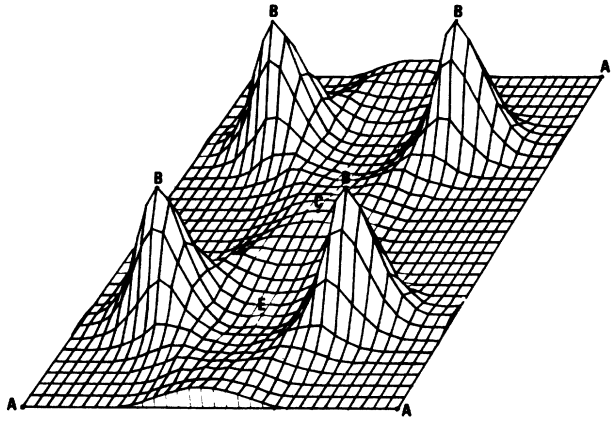

FIG. 3. Ag-ion density distribution in the (110) plane. Notations are the same as those in Fig. 2.

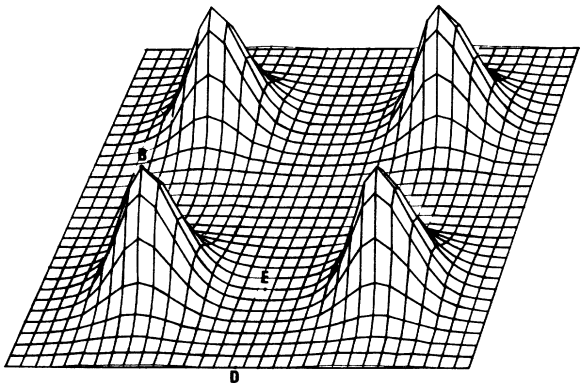

FIG. 4. Ag-ion density distribution in the $(\frac{1}{4}00)$ plane.

where the time averaging $\langle \cdots \rangle$ is to be understood as an average over time and the summations are over either anions or cations. The mean-square displacement was calculated for Te and Ag ions and is shown in Fig. 5 for several temperatures. The MSD of Ag ions increases with time, whereas that of the Te ions remains nearly constant. The linear regions in the functions $\langle r^2(t) \rangle_\alpha$ may be related to the diffusion coefficients D_α by the well-known equation

$$\langle r^2(t) \rangle_\alpha = 6D_\alpha t + C_\alpha \ , \tag{4}$$

where C_α is a constant term. The large-time behavior of the MSD shows that Ag ions have a large liquidlike self-diffusion coefficient. The asymptotic value of the MSD of Te ions is a measure of the Debye-Waller factor. From the gradient of the straight line in Fig. 5, the self-diffusion coefficient D_{Ag} of Ag ions is obtained for each temperature. These are shown in Fig. 6 with experimental results.[8] The temperature dependence agrees well with experiments.

When we plot $\ln D_{\mathrm{Ag}}$ against $1/T$, we see that it has Arrhenius-type behavior with a straight line. Then we can express the diffusion coefficient as follows:

$$D_{\mathrm{Ag}} = D_0 e^{-\varepsilon/k_B T} \ . \tag{5}$$

Here, D_0 is a constant with the dimension of the diffusion coefficient and k_B is Boltzmann's constant. The quantity ε denotes the activation energy for an ionic diffusion. From the gradient of the straight line of $\ln D_{\mathrm{Ag}}$ with Eq. (5), an ε value of 0.17 eV is obtained, which is in good agreement with the experimental value, 0.14 eV.[8]

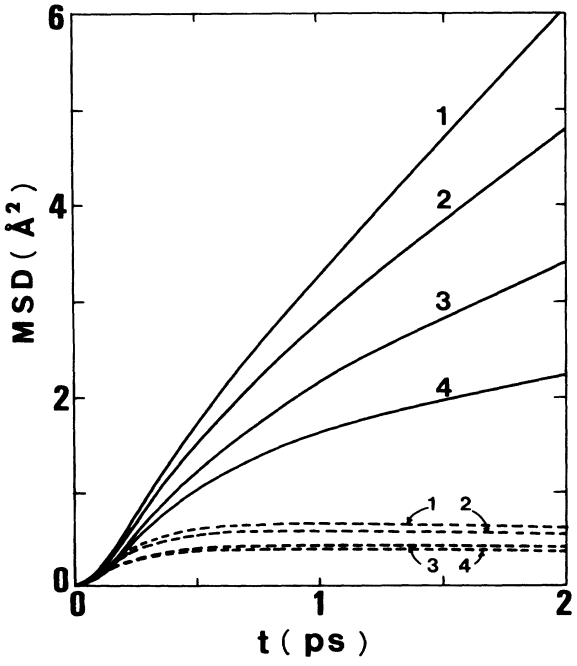

FIG. 5. Mean-square displacements of Ag ions (solid line) and Te ions (dotted line) at (1) $T=850$ K, (2) $T=750$ K, (3) $T=650$ K, and (4) $T=550$ K as a function of time.

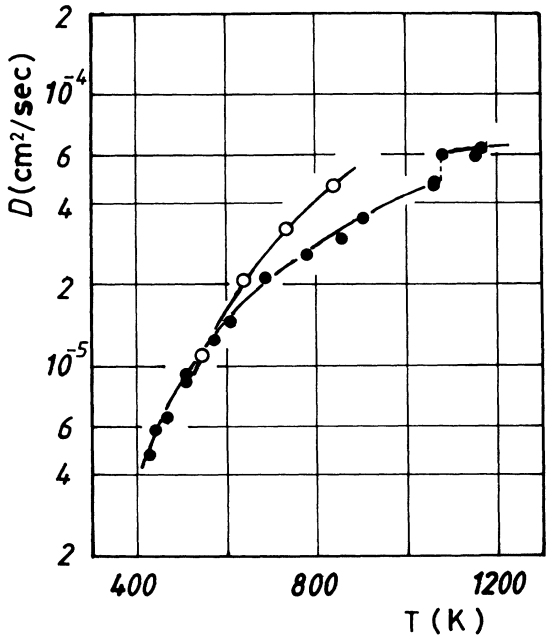

FIG. 6. Temperature dependence of the self-diffusion coefficient D_{Ag} of Ag ions. The MD results and experimental values (Ref. 8) are shown by the open circles and solid circles, respectively.

D. Velocity autocorrelation function

The normalized velocity autocorrelation functions for anions and cations are defined as

$$\Phi_\alpha(t) = \frac{\sum_{i=1}^{N_\alpha} \langle \mathbf{v}_i(t) \cdot \mathbf{v}_i(0) \rangle}{\sum_{i=1}^{N_\alpha} \langle \mathbf{v}_i(0) \cdot \mathbf{v}_i(0) \rangle}, \quad \alpha = \pm \ . \tag{6}$$

The Fourier transform $\Phi_\alpha(\omega)$ of the function $\Phi_\alpha(t)$ is given by

$$\Phi_\alpha(\omega) = \int_0^\infty \Phi_\alpha(t) e^{i\omega t} dt \ . \tag{7}$$

Then the self-diffusion coefficient D_α may also be related to the velocity autocorrelation function (VAF) by[5,6]

$$D_\alpha = \frac{k_B T}{M_\alpha} \int_0^\infty \Phi_\alpha(t) dt = \frac{k_B T}{M_\alpha} \Phi_\alpha(\omega = 0) \ . \tag{8}$$

The VAF's of the Ag and Te ions are shown in Fig. 7. It is quite characteristic that the VAF of Te shows a larger oscillating behavior than that of Ag. These reflect that Te ions retain their vibrating motion around the lattice sites, whereas Ag ions do their diffusive motion in a crystalline cage.

The Fourier transforms $\Phi_\alpha(\omega)$ are shown in Fig. 8. When the value of $\Phi_{\mathrm{Ag}}(\omega=0)$ is inserted into Eq. (8), we get $1.15(1.13) \times 10^{-5}$ cm^2/s at $T=550$ K and $4.70(4.62) \times 10^{-5}$ cm^2/s at $T=850$ K as the self-diffusion coefficient D_{Ag}. The numerical value in the parentheses corresponds to that obtained from the MSD. The two

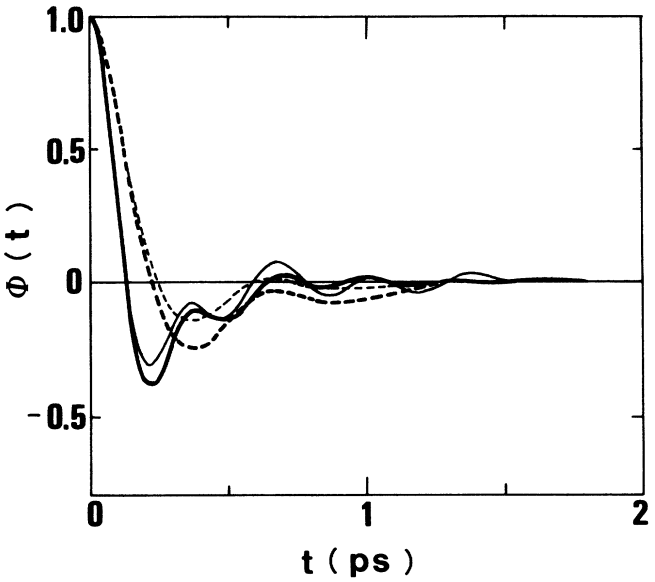

FIG. 7. VAF's of Ag ions (solid line) and Te ions (dotted line) at $T=550$ K (bold line) and $T=850$ K (thin line).

methods give more or less the same value. The numerical value of the diffusion coefficient obtained by differentiating MSD is more reliable than that obtained by integrating the VAF because of the truncation in the upper limit of the integral.

E. Current-current correlation function

In order to obtain the ionic conductivity, it is necessary to calculate the current-current correlation function. The normalized current-current correlation function is

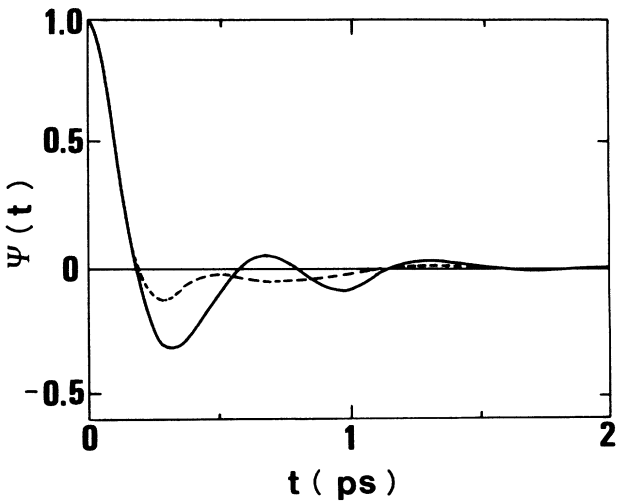

FIG. 9. Current-current correlation functions at $T=550$ K (solid line) and at $T=850$ K (dotted line).

defined by

$$\Psi(t)=\frac{\langle \mathbf{J}(t)\cdot\mathbf{J}(0)\rangle}{\langle \mathbf{J}(0)\cdot\mathbf{J}(0)\rangle} , \tag{9}$$

where $\mathbf{J}(t)$ is the charge current given by

$$\mathbf{J}(t)=e\left[\sum_{i=1}^{N_{\mathrm{Ag}}} z_{\mathrm{Ag}}\mathbf{v}_i(t)+\sum_{i=1}^{N_{\mathrm{Te}}} z_{\mathrm{Te}}\mathbf{v}_i(t)\right] . \tag{10}$$

$\Psi(t)$ and its Fourier transform $\Psi(\omega)$ are shown in Figs. 9 and 10. The ionic conductivity $\sigma(\omega)$ is given by the Kubo formula as follows:[6]

$$\sigma(\omega)=\frac{1}{3Vk_BT}\int_0^\infty \langle \mathbf{J}(t)\cdot\mathbf{J}(0)\rangle e^{i\omega t}dt , \tag{11}$$

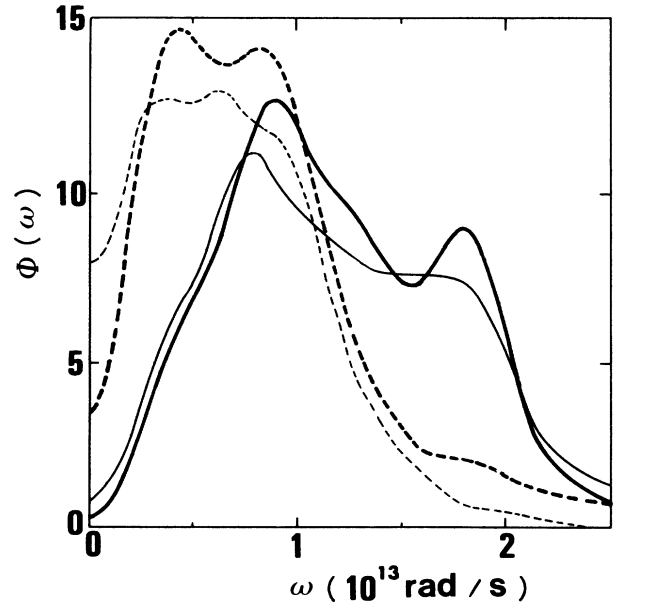

FIG. 8. Fourier transform of VAF's of Ag ions (solid line) and Te ions (dotted line) at $T=550$ K (bold line) and $T=850$ K (thin line).

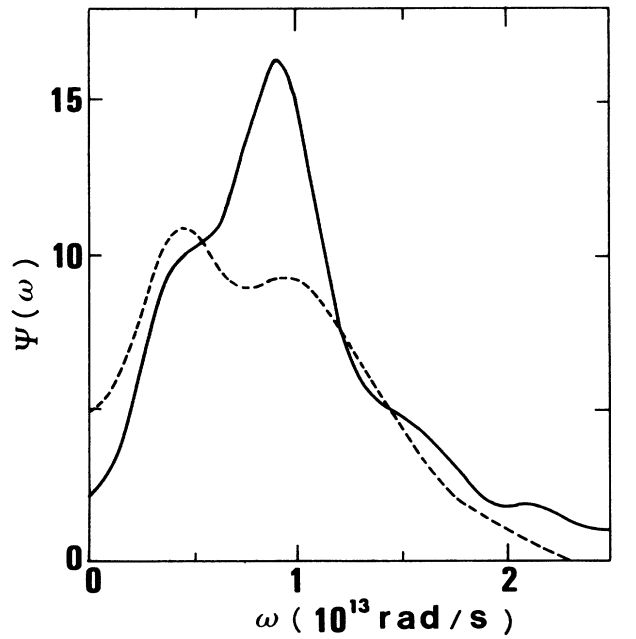

FIG. 10. Fourier transforms of current-current correlation functions at $T=550$ K (solid line) and at $T=850$ K (dotted line).

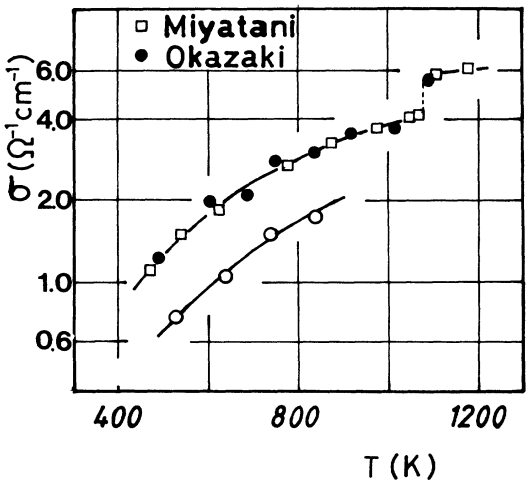

FIG. 11. Temperature dependence of static ionic conductivity $\sigma(0)$, shown by circles. Experimental values measured by Miyatani (Ref. 1) (squares) and Okazaki (Ref. 8) (solid circles) are also shown.

where V is the volume. The temperature dependence of static ionic conductivity $\sigma(\omega=0)$ is obtained, as shown in Fig. 11, with experimental values.[1,8] The tendency of temperature dependence is in good agreement with experiments.

Next we calculate the Haven's ratio H_R, which is defined by

$$H_R=\frac{D_{\mathrm{Ag}}}{D_\sigma}\ , \tag{12}$$

Here, D_σ is the diffusion constant obtained by using the Nernst-Einstein relation, is written as

$$D_\sigma=\frac{k_B T\sigma(0)}{n_{\mathrm{Ag}}(z_{\mathrm{Ag}}e)^2}\ , \tag{13}$$

where n_{Ag} is the Ag-ion density, N_{Ag}/V. We show Haven's ratio in Fig. 12 as a function of temperature. Experimental values of Okazaki[3] are also plotted. The MD results agree well with experiment. The difference from unity in Haven's ratio implies that this system has a deviation from the Nernst-Einstein relation.

The peak of $\sigma(\omega)$ is attributed to the transverse-optical–phonon mode in α-AgI-type superionic conductors. Figure 10 gives 82 cm^{-1} the transverse-optical–phonon frequency.

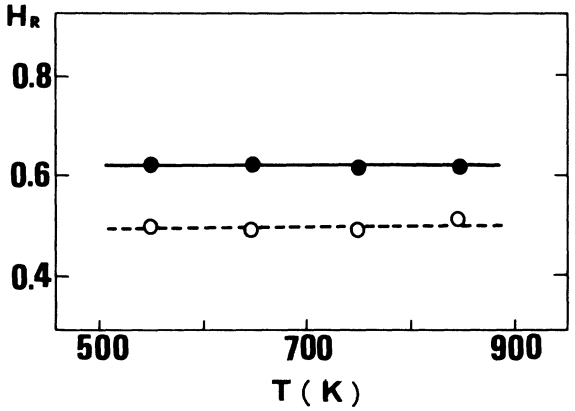

FIG. 12. Calculated temperature dependence (circles) of Haven's ratio are plotted with experiments (Ref. 3) (solid circles).

IV. CONCLUSIONS

We have done the MD simulation for the superionic conductor α-Ag_2Te. Calculated quantities such as the radial distribution functions, the density distribution of Ag ions, the self-diffusion coefficient of Ag ions, D_{Ag}, the ionic conductivity, Haven's ratio, and the activation energy are in good agreement with experiment. These facts ensure the validity of the present model of α-Ag_2Te we are dealing with.

Finally, we emphasize that the Ag ions in Ag_2Te do not jump from tetrahedral site to tetrahedral site directly on the $(\frac{1}{4}00)$ plane, but jump from tetrahedral site to tetrahedral site through the vicinity of the octahedral site along zigzag paths.

ACKNOWLEDGMENTS

The authors wish to express their thanks to Professor A. Ueda for his useful instruction regarding the MD simulation technique. They would like to acknowledge Professor S. Tamaki for his critical reading of the manuscript. They also wish to thank Dr. Y. Kaneko for his helpful discussions. They are indebted to the Information Processing Center of Niigata University for the allocation of a large amount of computing time on the ACOS-S850 computer.

[1]S. Miyatani, J. Phys. Soc. Jpn. **13**, 341 (1958); S. Miyatani and I. Yokota, *ibid.* **14**, 750 (1959).
[2]I. Yokota, J. Phys. Soc. Jpn. **21**, 420 (1966).
[3]H. Okazaki, J. Phys. Soc. Jpn. **23**, 355 (1967); **43**, 213 (1977).
[4]See, for example, G. D. Mahan and W. L. Roth, *Superionic Conductors* (Plenum, New York, 1976).
[5]M. J. L. Sangster and M. Dixon, Adv. Phys. **25**, 247 (1976).
[6]A. Rahman and P. Vashishta, in *The Physics of Superionic Conductors and Electrode Materials*, edited by J. W. Perran (Plenum, New York, 1983), p. 93.
[7]H. Matsuda and Y. Hiwatari, in *Cooperative Phenomena*, edited by H. Haken and M. Wagner (Springer-Verlag, Berlin, 1973), p. 250.
[8]H. Okazaki (unpublished).
[9]T. Sakuma and S. Saitoh, J. Phys. Soc. Jpn. **54**, 3647 (1985).
[10]K. Koto, H. Schulz, and R. A. Huggins, Solid State Ionics **1**, 355 (1980).
[11]M. H. Dickens, W. Hayes, M. T. Hutchings, and C. Smith, J. Phys. C **15**, 4043 (1982).
[12]A. B. Walker, M. Dixon, and M. J. Gillan, J. Phys. C **15**, 4061 (1982).
[13]M. J. Gillan, Physica **131B**, 157 (1985).
[14]Y. Kaneko and A. Ueda, J. Phys. Soc. Jpn. (to be published).